

## Self-nucleation-induced nonisothermal crystallization of nylon 6 from the melt

Huizhen Li,<sup>1,2</sup> Ran Guo,<sup>2</sup> Yuhai Liu,<sup>2</sup> Shaoxuan Liu,<sup>2</sup> Edyta Proniewicz,<sup>3,4</sup> Leonard M. Proniewicz,<sup>3</sup> Ying Zhao,<sup>5</sup> Yizhuang Xu,<sup>2</sup> Jinguang Wu<sup>2</sup>

<sup>1</sup>School of Chemistry and Chemical Engineering, Henan Normal University, Xinxiang 453007, People's Republic of China

<sup>2</sup>College of Chemistry and Molecular Engineering, Peking University, Beijing 100871, People's Republic of China

<sup>3</sup>Faculty of Chemistry, Jagiellonian University, ul. Ingardena 3, 30-060 Krakow, Poland

<sup>4</sup>Faculty of Foundry Engineering, AGH University of Science and Technology, ul. Reymonta 23, 30-059 Krakow, Poland

<sup>5</sup>Institute of Chemistry, Chinese Academy of Sciences, Beijing 100190, People's Republic of China

Correspondence to: Yizhuang Xu (E-mail: xyz@pku.edu.cn)

**ABSTRACT:** The effect of thermal treatment over a wide range of temperature (130–280°C) on the crystallization behavior of nylon 6 was studied by using DSC, FTIR, and polarized light microscope equipped with a hot stage. The crystallization and the subsequent melting behavior of the nylon 6 samples treated at different temperatures ( $T_s$ ) were classified into four types. When  $T_s$  was higher than 236°C or lower than 213°C, the crystallization behavior of nylon 6 was insensitive to the variation of  $T_s$ . When  $T_s$  was in the range of 213–235°C, the crystallization behavior was sensitive to the change of  $T_s$ . The polarized light microscopic experiments have demonstrated that a large amount of tiny ordered nylon 6 segments/cluster persisted when nylon 6 film are heated to 231°C. Consequently, the fastest crystallization speed was observed. As  $T_s$  was between 214 and 223°C, both the  $T_m$  and the  $\Delta H_m$  were higher than those of the nylon 6 samples treated at other temperature. The polarized light microscopic investigations have also demonstrated that molten nylon 6 crystallizes by using the un-molten nylon 6 crystals as nucleation center at 220°C. Crystallization at higher temperature produces nylon 6 with thicker crystalline lamella. The above results are helpful for rational design of thermal treatment procedure to obtain nylon 6 with different crystalline features. © 2015 Wiley Periodicals, Inc. *J. Appl. Polym. Sci.* **2015**, *132*, 42413.

**KEYWORDS:** crystallization; phase behavior; polyamides

Received 30 March 2014; accepted 23 April 2015

DOI: 10.1002/app.42413

### INTRODUCTION

Nylon 6 (polycapramide) is a high-performance semi-crystalline synthetic polyamide, which has found wide applications in the field of synthetic fibers and engineer plastics.<sup>1–4</sup> It is generally recognized that macroscopic properties of semi-crystalline polymers, such as nylon 6, are governed by their microscopic structural features such as crystalline structure, morphology, which in turn, are closely related to the processing procedures.<sup>5–9</sup> Because of the close relationship between the processing procedures and microscopic structure of nylon 6, a large amount of work on intervening the crystallization of nylon has been accumulated over the years. For example, nonisothermal or isothermal crystallization behavior of nylon and its relevant materials, such as composites,<sup>2,10–14</sup> copolymers,<sup>15</sup> or blends<sup>16–18</sup> have been extensively investigated to improve their performance. In our previous work,

we have introduced metal ions, including lanthanide into nylon 6 matrix to improve the spinnability of nylon 6. As a result, super-fine nylon 6 filaments have been successfully manufactured.<sup>4,14,19</sup>

In addition, we have also proposed a new approach to prepare nylon 6 with high crystallinity and special morphological feature.<sup>20</sup> The resultant nylon 6 possesses bright perspective in developing bioreactors.<sup>20,21</sup>

In most cases, nylon products are manufactured by melting processing. Crystallization from nylon 6 melt is under the control of nucleation and the crystal growth. Because the nucleation kinetics exhibits a significant impact upon the bulk properties and processability of polymer materials, methods to control nucleation are of great academic and industrial relevance. Self-nucleation is now used as a general term to describe nucleation of a macromolecular melt or solution by its own crystals grown previously.

This article was published online on 6 June 2015. An error was subsequently identified. This notice is included in the online and print versions to indicate that both have been corrected 30 June 2014.

© 2015 Wiley Periodicals, Inc.

Self-nucleation has much influence on polymer morphology, crystal form, and polymer properties because there is a wide temperature range where un-molten crystallites and molten polymer co-exist.<sup>22</sup> Over the past decades, self-nucleation has been extensively used to affect crystallization behavior of polymers, polymer blends, and block copolymers.<sup>23–29</sup>

Fillon *et al.*<sup>30–32</sup> have demonstrated that self-nuclei can be generated in a controlled fashion by using suitable self-nucleation annealing protocols in a DSC experiment. The experimental protocol developed by Fillon is composed of four steps: (a) Erasure of previous history: the sample is heated well above its melting temperature to erase the previous thermal history; (b) Creation of “Standard” initial state: the polymeric material is cooled down to a temperature well below the normal crystallization range so that a “standard” initial state is obtained; (c) Self-nucleation: the polymeric material is heated to selected temperature ( $T_s$ ) and kept at  $T_s$  for a pre-set time. This step results in partial melting and the formation of annealed crystal fragments; (d) Final Crystallization: the sample is cooled down so that the un-molten crystal fragments can induce molten polymer to crystallize; (e) Final melting: as an optional step, a final melting of the sample can be used as a means to check the thermal stability of the sample. The Fillon’s approach is expected to be helpful in enhancing our understanding of the crystallization of nylon 6 under the influence of self-nucleation. To the best of our knowledge, there is no report on the crystallization behavior of neat nylon 6 by using the Fillon’s approach in the literature. This study is an attempt to gain insight into the nonisothermal crystallization behavior of nylon 6 under the influence of the self-nucleation.

## EXPERIMENTAL

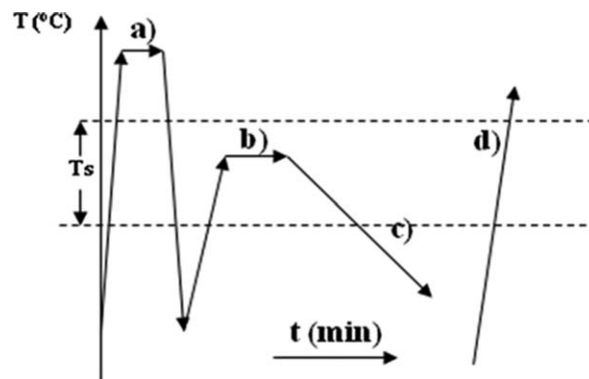
### Materials

A commercial grade of nylon 6 was supplied by Yue-yang Petrochemical Cooperation. The relative viscosity of nylon-6 is 3.35, which is corresponding to a viscous average molecular weight of  $2.65 \times 10^4$ .

### Instruments and Techniques

A TA Q100 instruments (New Castle, DE) equipped with a Refrigerated Cooling System (RCS) was used. Samples were encased in aluminum pans, and a vacant aluminum pan was used as a reference. The weights of all samples for DSC (Differential Scanning Calorimetry) measurements were around 5.0 mg. A purging gas (nitrogen, 100 mL/min) was used to prevent oxidation of nylon sample during thermal measurement.

The thermal treatment protocol was composed of four steps (Scheme 1): (a) the initial nylon 6 samples were heated at a heating rate of 10°C/min to 280°C (about 60°C above the observed melting point of nylon 6) and kept at 280°C for 5 min to erase the previous history. Then, the samples were cooled down to 80°C at a cooling rate of 10°C/min so that a “standard” initial state is obtained. (b) Each nylon 6 sample was heated to pre-set temperature (the pre-set temperature is denoted as  $T_s$  and the range of  $T_s$  is from 130 to 280°C) at a heating rate of 10°C/min and kept at  $T_s$  for 15 min. (c) The nylon 6 sample was subsequently cooled down to 120°C at a cooling rate of 1°C/min. (d) The obtained samples were heated



**Scheme 1.** Scheme for the heat treatment: (a) heating to 280°C and held for 5 min to erase the former thermal history and then cooled down to 80°C to create the initial “standard” state; (b) heating to the selected temperature ( $T_s$ ) (10°C/min), annealing (15 min), the  $T_s$  ranges from 150 to 280°C. (c) cooling from  $T_s$  (1°C/min, crystallization after self-nucleating), and (d) final melting (10°C/min, DSC).

to 280°C at a heating rate of 10°C/min so that the resulting DSC thermograms can be used to characterize the crystallization behavior of nylon 6 sample treated at different  $T_s$ .

FTIR spectra of the nylon 6 samples were recorded on a Nicolet Magna 750 FT-IR spectrometer with a NIC-Plan microscope equipped with a liquid nitrogen-cooled mercury-cadmium telluride (MCT) detector. For each measurement, 128 scans were co-added at a spectral resolution of 2  $\text{cm}^{-1}$ .

Polarized light microscopy observation was used to register crystallization changes in terms of transmitted light during heating and cooling process by using a Leica DMLP polar microscope with a hot stage.

Nylon 6 film with thickness ca. fifty micrometers was placed between two glass slides. During the heating and cooling process, the micrographs of the sample under the polarized microscope were recorded by using a digital camera.

## RESULTS AND DISCUSSION

To some extent, DSC experiment can reflect the melting and crystallization behavior of polymer effectively.<sup>33–35</sup>

Based on DSC experimental data, onset temperature of crystallization, crystallization temperature, crystalline enthalpy, onset temperature of melting, melting temperature, melting enthalpy of nylon 6 pretreated at different  $T_s$  are obtained and summarized in Table I. According to the data shown in Table I, the nylon 6 samples can be classified into four types as  $T_s$  changes.

Samples with  $T_s$  higher than 236°C are classified as the first type. As shown in Figure 1(a), each DSC trace is composed of a main crystalline peak at about 191°C and a shoulder at about 197°C. The crystalline enthalpy is about 70–76 J/g. In the subsequently heating process, two broad overlapping melting peaks at about 215 and 217°C are observed. [Figure 1(b)] The peak at 215°C is stronger than that at 217°C. The melting enthalpy is about 70–77 J/g, which is roughly the same as the crystalline enthalpy in the cooling process.

To shed light on the relationship between the crystalline peaks in Figure 1(a) and melting peaks illustrated in Figure 1(b), the

**Table I.** Thermal Analysis Data of Nylon 6 Pretreated at Different  $T_s$ 

$T_s$ (°C)	Onset temperature of $T_c$ (°C)	$T_c$ (°C)	$\Delta H_c$ (J/g)	Onset temperature of $T_m$ (°C)	$T_m$ (°C)	$\Delta H_m$ (J/g)
130	130			196	139; 220	64.18
140	140			199	147; 220	58.30
150	150			201	158; 220	67.88
160	160			201	166; 220	71.10
170	170			202	177; 220	70.22
180	180			203	186; 220	71.54
190	190			191; 205	196; 220	73.47
200	200			201; 214	210; 220	75.99
205	205			206; 217	213; 220	80.34
207	207			209	215; 219	82.76
208	208			210	215; 219	84.36
209	209			210	216; 218	85.77
210	210			212	219	95.15
213	213			215	221	88.28
214	214			215	222	89.57
215	215			215	223	84.97
216	216			217	223	76.42
217	217			217	224	93.31
218	218			219	224	101.00
219	219			190; 221	216; 224	98.40
220	220	204, 214	49.78	193; 222	218; 225	88.56
221	210	203	38.56	194; 222	219; 225	94.04
222	210	203	50.14	195; 224	220; 226	89.58
223	209	202	53.18	195; 225	219; 226	88.59
224	208	202	61.51	218	220	80.09
225	207	202	56.54	192	219	74.10
227	205	201	56.58	196	219	75.24
230	203	199	82.63	196	218	75.61
232	202	198	79.24	193	218	89.06
233	201	197	80.54	192	217	78.07
235	201	194	77.51	190	216	77.12
236	201	192	54.92	164.62	216	71.53
237	201	192	69.19	164.16	216	74.28
240	201	191	72.89	163.89	216	76.82
260	201	191	75.48	164.84	216	76.84
280	200	190	73.98	154.90	216	69.84

following DSC experiment was performed: Two nylon 6 samples were heated to 280°C at a heating rate of 10°C/min, and then kept at that temperature for 5 min to erase the previous thermal history. Subsequently, the two nylon 6 samples were cooled down to 80°C at a cooling rate of 10°C/min to obtain two standard samples. The obtained two nylon 6 samples are denoted as sample R and sample S, respectively.

In the next step, the sample S was heated to 280°C at a heating rate of 10°C/min, kept at 280°C for 15 min, and cooled down to 195°C at a cooling rate of 1°C/min. The sample R was heated

to 280°C at a rate of 10°C/min, kept for 15 min, and then cooled down to 120°C at a rate of 1°C/min. At last, both R and S samples were heated to 280°C at a rate of 10°C/min. The melting behaviors of sample R and sample S during the last heating procedures are shown in Figure 1(c). For sample S, the crystallization process occurring at 197°C was allowed, whereas the crystallization process at 191°C was prohibited. As shown in Figure 1(c), only one broad melting peak at about 217°C is observed in the last melting process of sample S. For sample R, crystallization processes at both 191 and 197°C are allowed. As

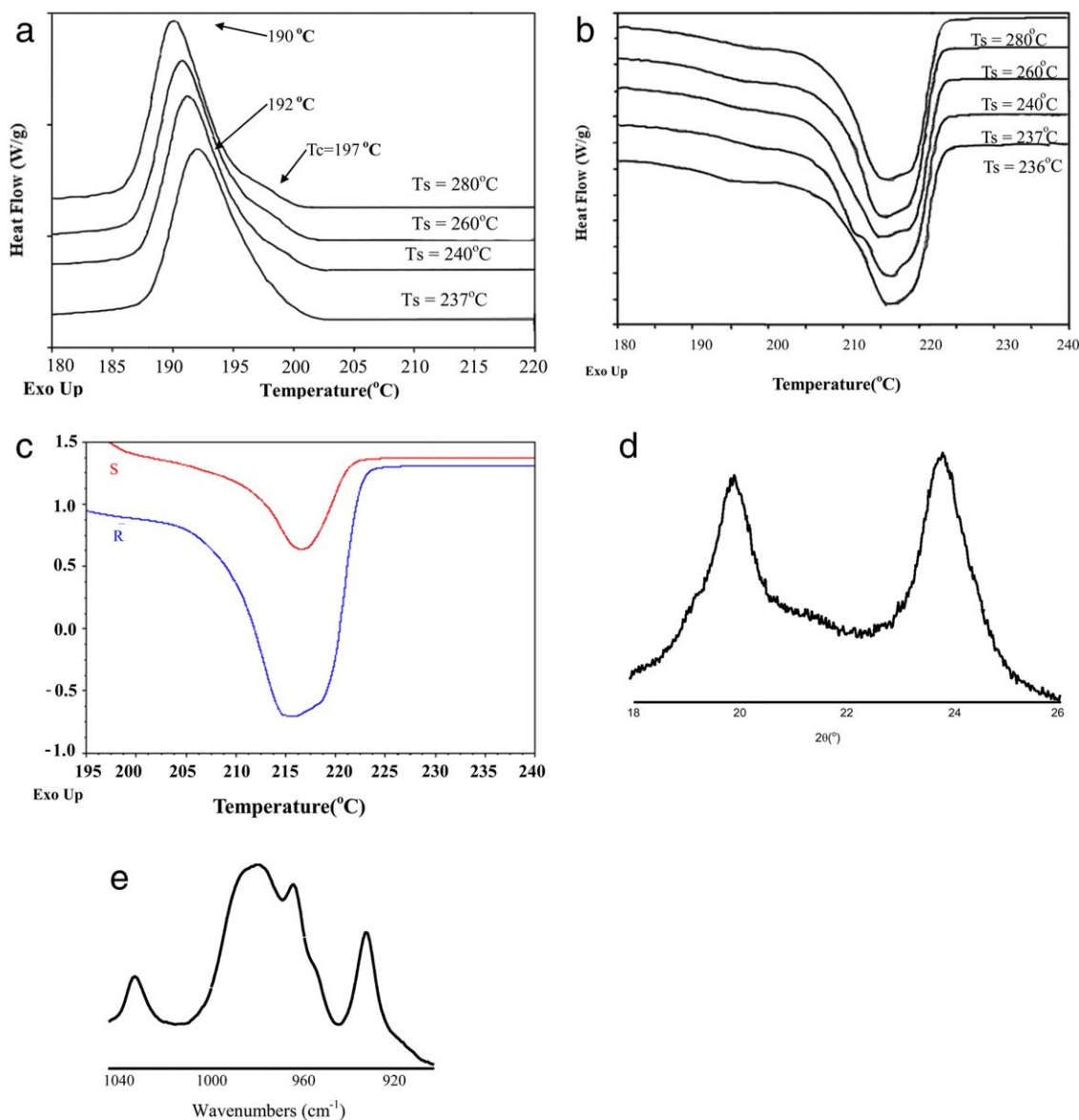


**Figure 1.** (a) The crystallization curves of the first type nylon 6 ( $T_s \geq 236^\circ\text{C}$ ). (b) The melting curves of the first type nylon 6 ( $T_s \geq 236^\circ\text{C}$ ). (c) The melting curves of the R and S samples ( $T_s \geq 236^\circ\text{C}$ ). (d) A typical XRD curve of the first type of nylon 6 sample. (e) A typical FTIR Spectrum of the first type of nylon 6 ( $T_s \geq 236^\circ\text{C}$ ). [Color figure can be viewed in the online issue, which is available at [wileyonlinelibrary.com](http://wileyonlinelibrary.com).]

a result, two broad overlapping melting peaks at about 215 and 217°C can be observed. The above results suggest that the nylon 6 crystal formed at 197°C corresponds to the one melting at 217°C.

Figure 1(d) shows WAXD patterns of a typical nylon 6 sample. Two peaks at about 20° and 24°, which are assigned to the (200) and (002/202) reflections of  $\alpha$  nylon-6,<sup>35</sup> can be observed. It is clear that no  $\gamma$  phase formed because the characteristic peak at 21° is not observable.<sup>36</sup>

A typical FTIR spectrum of the first type of the nylon 6 sample shown in Figure 1(e) also demonstrates that the first type of nylon 6 is dominated by  $\alpha$ -form. A series of characteristic bands at 1030, 960, and 930  $\text{cm}^{-1}$  of nylon 6 in  $\alpha$ -form can be observed.<sup>37</sup> In addition, a strong broad absorption which can be

attributed to amorphous nylon 6 is observed at around 980  $\text{cm}^{-1}$ . However, the characteristic spectral features for nylon 6 in  $\beta$  or  $\gamma$  forms are too weak to be detected [Figure 1(e)]. The above results demonstrate that nylon 6 in  $\alpha$ -form is dominating crystalline phase in the nylon 6 samples.

As shown in Figure 1(a), the crystallization temperature (denoted as  $T_c$ ) is insensitive to the  $T_s$  changes. Here, we discuss the DSC behavior of two typical nylon 6 samples whose  $T_s$  are 237 and 280°C, respectively. The main crystallization peak (at about 192°C) alters only about 2°C although the difference on  $T_s$  is almost 50°C. Thus, we believe that the nylon 6 crystallites are almost completely destroyed when  $T_s$  is higher than 236°C. The absence of the residual nylon 6 crystallites in the melt results in no self-nucleation effect. Thus, the crystallization



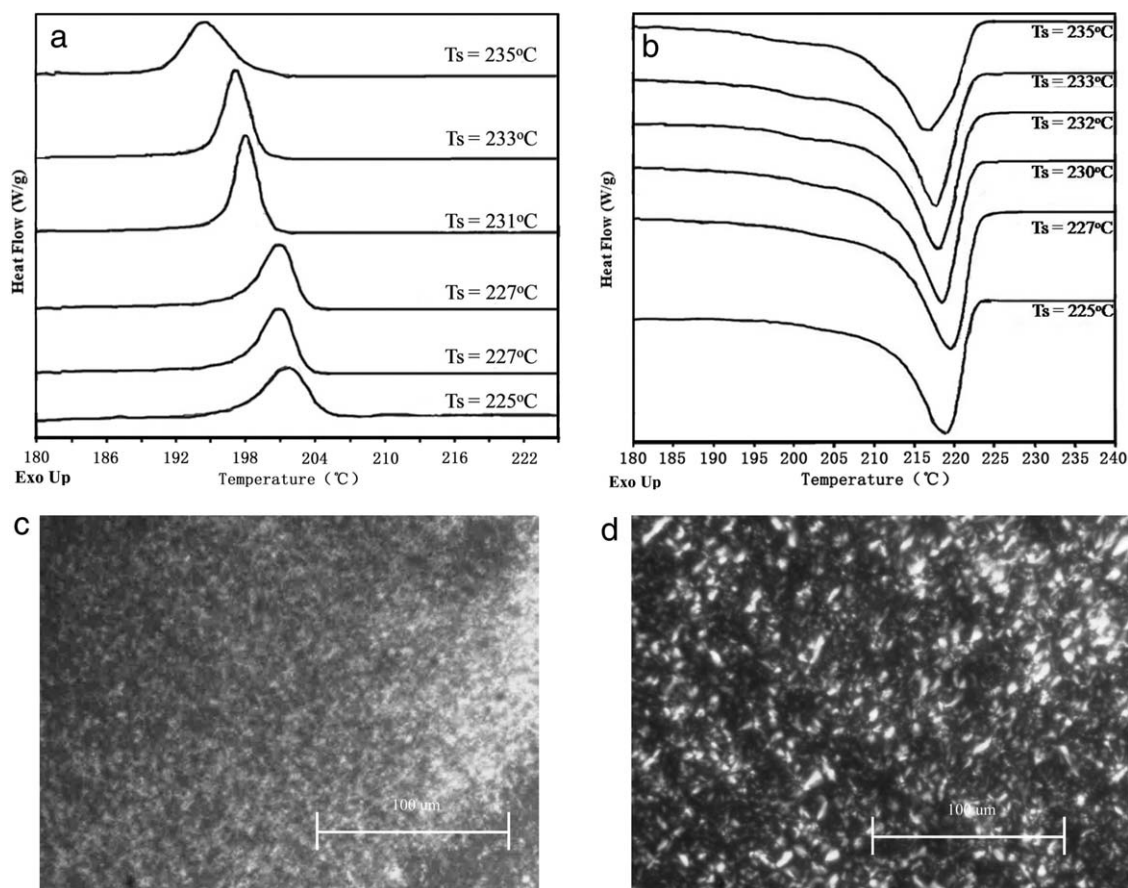


**Figure 2.** (a) The crystallization curves of the second type of nylon 6 samples ( $T_s = 224\text{--}235^\circ\text{C}$ ). (b) The melting curves of the second type nylon 6 samples ( $T_s = 224\text{--}235^\circ\text{C}$ ). (c) Optical micrograph of a nylon 6 sample during the cooling process ( $T_s$  is  $231^\circ\text{C}$ ). (d) Optical micrograph of a nylon 6 sample during the cooling process ( $T_s$  is  $250^\circ\text{C}$ ).

behavior and the subsequent melting behavior are insensitive to the variation of  $T_s$ .

Samples with  $T_s$  in the range of  $224\text{--}235^\circ\text{C}$  can be classified as the second type of nylon 6. As is shown in Figure 2(a), only one crystallization peak can be observed in each DSC trace. The crystallization enthalpy is about  $54\text{--}82$  J/g. In the heating process, only a single melting peak can be observed in each DSC trace [Figure 2(b)]. The melting enthalpy ranges from  $74$  to  $89$  J/g and is larger than that of the crystallization enthalpy in the third step. The above results suggest that considerable amount of the nylon 6 ordered segments/crystallites persisted or formed when the nylon 6 sample was heated to  $T_s$  and kept at  $T_s$  for 15 min ( $T_s$  is between  $224$  and  $235^\circ\text{C}$ ). These nylon 6 ordered segments/crystallites act as nucleation centers and play an important role in affecting the crystallization behavior of nylon 6 during subsequent cooling process. The crystallization behavior of the second type of nylon 6 shown in Figure 2(a) is different from that of the first type in the following aspects:

(1)  $T_c$  of the second type of nylon 6 samples ( $194\text{--}202^\circ\text{C}$ ) were higher than that of the first type of nylon 6 samples ( $191^\circ\text{C}$ ); 2) upon increasing  $T_s$  from  $224$  to  $235^\circ\text{C}$ , the crystallization peak exhibits a significantly shifts toward lower temperature; and (3)

with increasing of the  $T_s$ , the width of the crystallization peak decreases first and then increases. When  $T_s = 231^\circ\text{C}$ , the crystallization peak becomes the narrowest, which indicates that the crystallization rate is the fastest.

To understand why the crystallization rate became the fastest, polarized light microscopic experiment was used to study the crystallization process of nylon 6 treated at different  $T_s$ . Two nylon 6 films were first heated to  $280^\circ\text{C}$  at a heating rate of  $10^\circ\text{C}/\text{min}$  and kept for 5 min to remove previous thermal history. Then, the samples were cooled down to  $80^\circ\text{C}$  at a cooling rate of  $10^\circ\text{C}/\text{min}$ , so that “standard” states were obtained. In the next step, one nylon 6 film was heated to  $231^\circ\text{C}$  at a heating rate of  $10^\circ\text{C}/\text{min}$  and kept at  $231^\circ\text{C}$  for 15 min. Another nylon 6 film was heated to  $250^\circ\text{C}$  at the heating rate of  $10^\circ\text{C}/\text{min}$  and kept at  $250^\circ\text{C}$  for 15 min. In the subsequent cooling process, at a cooling rate of  $1^\circ\text{C}/\text{min}$ , these two nylon 6 samples exhibit markedly different crystallization behavior. For the nylon 6 film treated at  $231^\circ\text{C}$ , large amount of tiny crystallites appeared simultaneously when the temperature reaches  $209^\circ\text{C}$  [Figure 2(c)]. Although the brightness of the micrograph of the nylon 6 film increased in the subsequent cooling process, the size of crystallites exhibited insignificant variation. For the nylon 6 film whose  $T_s$  is  $250^\circ\text{C}$ , bright nylon 6 crystallites appeared sporadically when the temperature reached  $207^\circ\text{C}$

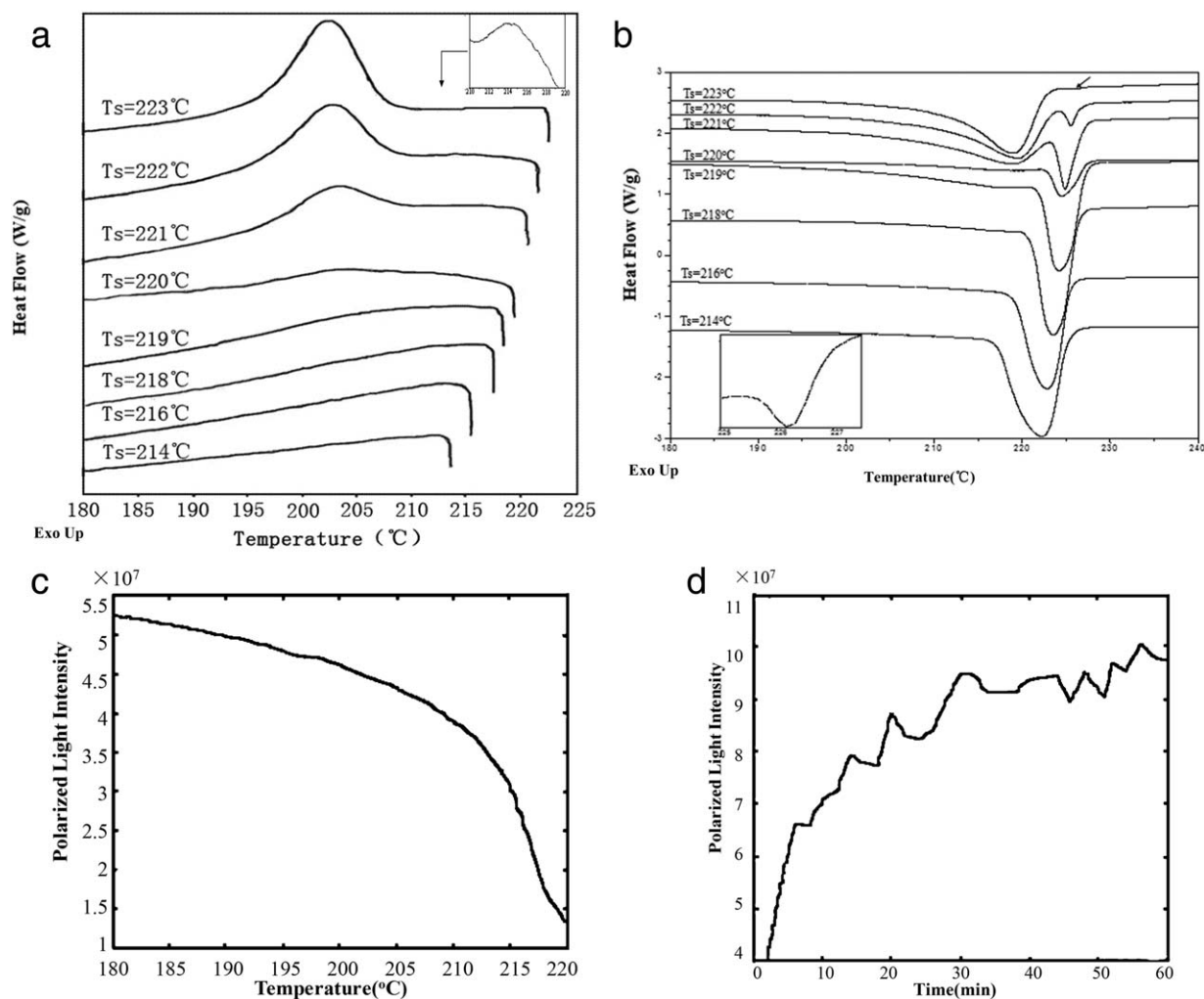


**Figure 3.** (a) The crystallization curves of the third type of nylon 6 samples ( $T_s = 214$ – $223^\circ\text{C}$ ) (In-set is a weak peak marked by an arrow). (b) The melting curves of the third type nylon 6 samples ( $T_s = 214$ – $223^\circ\text{C}$ ) (In-set is a weak peak marked by an arrow). (c) The variation of the intensity of polarized light as a function of time when the nylon 6 sample is heated to  $220^\circ\text{C}$ . (d) The variation of the intensity of the polarized light as a function of annealing time when the nylon 6 sample is kept at  $220^\circ\text{C}$ .

[Figure 2(d)]. The size of nylon 6 crystallites increased slowly in the following cooling process. The above results demonstrate that large amount of the tiny ordered nylon 6 segments/crystallites are produced when  $T_s$  is  $231^\circ\text{C}$ . The tiny ordered nylon 6 segments/crystallites make crystallization *via* self-nucleation mode occur simultaneously. As a result, crystallization with the largest rate was obtained during the cooling process.

Samples with  $T_s$  in the range of  $214$  to  $223^\circ\text{C}$  are classified as the third type. As shown in Figure 3(a), two crystallization peaks at ca.  $204^\circ\text{C}$  and ca.  $214^\circ\text{C}$  are observed. Two melting peaks (at about  $220^\circ\text{C}$  and  $225$ – $227^\circ\text{C}$ ) are seen in the subsequent heating process [Figure 3(b)]. The melting enthalpies are about  $76$ – $101$  J/g. The characteristic crystallization behaviors of the third type of the nylon 6 samples are as follows: (1)  $T_c$  of the third type of nylon 6 is higher than that of the first two types of nylon 6. (2) As  $T_s$  increases, the intensity of the  $204^\circ\text{C}$  peak increases, whereas the intensity of the crystallization peak at about  $214^\circ\text{C}$  decreases. (3) In comparison with the first and the second types of nylon 6 samples, the melting temperature

and melting enthalpies of the third types of the nylon 6 samples are much higher. It should be pointed out that the melting temperature of nylon crystallites is higher than the apparent melting point of nylon 6.

To enhance our understanding on the crystallization behavior of the third type of the nylon 6 samples, the following polarized microscopic experiments were performed. An initial nylon 6 sample was first heated to  $280^\circ\text{C}$  at a heating rate of  $10^\circ\text{C}/\text{min}$  and kept for 5 min to remove previous thermal history. Then, the sample was cooled down to  $80^\circ\text{C}$  at a cooling rate of  $10^\circ\text{C}/\text{min}$ , so that “standard” initial state was obtained. Subsequently, this sample was heated to  $220^\circ\text{C}$  at a heating rate of  $10^\circ\text{C}/\text{min}$  and anneal at  $220^\circ\text{C}$  for 1 h. During the heating and annealing process, electronic photographs of the nylon 6 film under polarized light microscope were recorded. The recorded electronic micrographs were converted into the black–white mode. Then, the summation of the brightness of each pixel in the electronic micrograph was used to reflect the intensity of transmitted light. The calculation was performed by using a program for MATLAB

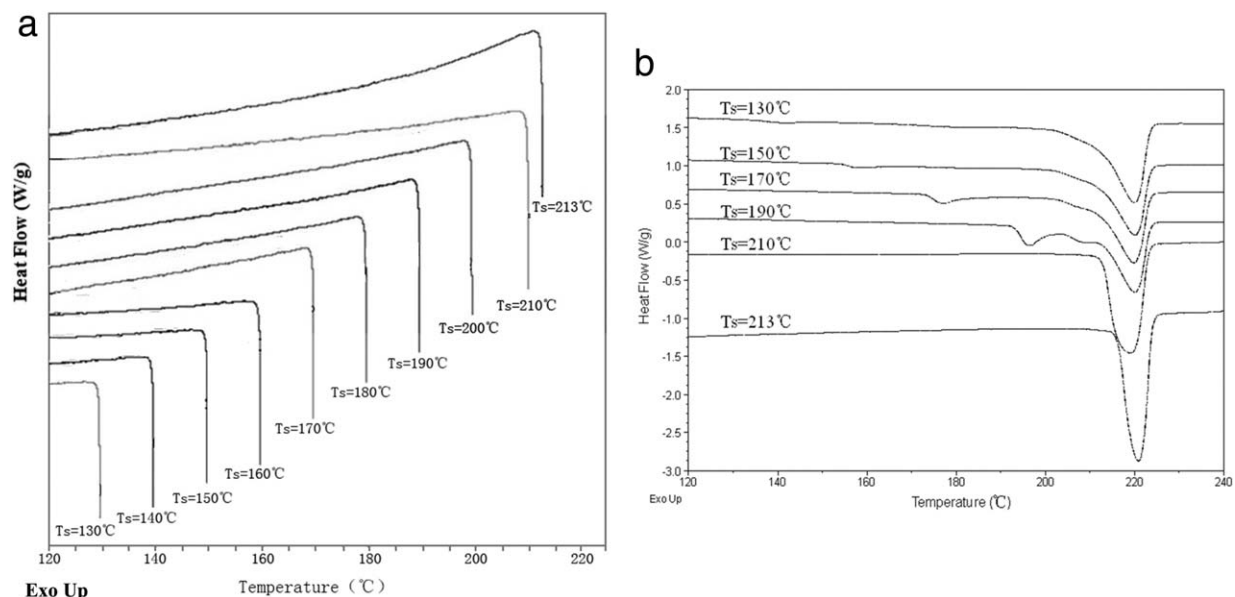


**Figure 4.** (a) The crystallization curves of the fourth type nylon 6 sample ( $T_s = 130\text{--}213^\circ\text{C}$ ); (b) The melting curves of the fourth type nylon 6 sample ( $T_s = 130\text{--}213^\circ\text{C}$ ).

(The Math Works Inc.) written in our laboratory. Figure 3(c) shows the changes of the transmitted light intensity as a function of temperature during the heating process. The intensity of the transmitted light decreases as the temperature increases. However, the intensity of the transmitted light did not reach zero when the temperature amount to  $220^\circ\text{C}$ . This phenomenon demonstrates that the nylon 6 sample did not melt completely and there were considerable amount of the nylon 6 crystallites left.

Figure 3(d) illustrates the variation of the transmitted light intensity as a function of annealing time when nylon 6 was annealed at  $220^\circ\text{C}$ . The intensity of the transmitted light increases upon increasing the annealing time. That is to say, molten nylon 6 underwent crystallization by using the un-molten nylon crystallites as nucleation center when the nylon 6 film was annealed at  $220^\circ\text{C}$ . As a result, the crystallization temperature is much higher than those of the first and the second type of the nylon 6 samples. The high crystallization temperature produced the nylon 6 crystallites with increasing thickness of the crystalline lamella. According to the Thomson-Gibbs, eq. (1),<sup>38</sup> thicker crystalline lamellae confer the nylon 6 sample with a sharp peak whose melting temperature (around  $225^\circ\text{C}$ ) is higher than the apparent melting point ( $220^\circ\text{C}$ ) of nylon 6.

$$T_m = T_m^0 [1 - (2\delta/l\Delta H_f)] \quad (1)$$

( $T_m$ : melting temperature;  $T_m^0$ : equilibrium melting temperature;  $\delta$ : the origin of the folded surface free energy;  $l$ : thickness of lamella,  $\Delta H_f$ : full melting enthalpy).

Finally, the fourth type of the nylon 6 samples was acquired when  $T_s$  is in the range of  $130\text{--}213^\circ\text{C}$ . As shown in Figure 4(a), the DSC curves exhibit somewhat concave in shape, suggesting that there is a broad crystalline peak. We suggest that crystallization occurred immediately upon decreasing the temperature. Furthermore, the feature of the crystallization peak is almost invariant as  $T_s$  changes, indicating that the crystalline

speed was insensitive to  $T_s$ . Figure 4(b) shows the DSC traces of the fourth type of nylon 6 samples in the heating process. In most cases, two melting peaks were observed. One is the main melting peak at ca.  $220^\circ\text{C}$ , and another was a pre-melting peak. The main melting peak does not change significantly as  $T_s$  varies, whereas the pre-melting peak moved toward high temperature and became more intense as  $T_s$  increases. When  $T_s$  is between  $210$  and  $213^\circ\text{C}$ , the pre-melting peak merged with the main melting peak and only one broad melting peak can be observed. Second derivative of the melting peak indicates that the broad melting peak is composed of two peaks at about  $218$  and  $220^\circ\text{C}$ .

## CONCLUSION AND PERSPECTIVE

This study examined the effects of the thermal treatment in a wide temperature range on the crystallization behavior of nylon 6. The crystallization and the subsequent melting behavior of the nylon 6 samples could be classified into four types. When  $T_s$  is higher than  $236^\circ\text{C}$  (the first type) or lower than  $213^\circ\text{C}$  (the fourth type), the crystallization behavior of nylon 6 is insensitive to the variation of  $T_s$ . As  $T_s$  is between  $213$  and  $235^\circ\text{C}$ , the crystallization behavior of nylon 6 is sensitive to the change of  $T_s$ . The polarized light microscopic experiments demonstrate that large amount of tiny ordered nylon 6 segments/cluster persist when  $T_s$  is set as  $231^\circ\text{C}$ . Consequently, the speed of crystallization is the fastest during the cooling process. For  $T_s$  between  $214$  and  $223^\circ\text{C}$  (the third type of nylon 6), both  $T_m$  and  $\Delta H_m$  are higher than those of the nylon 6 samples treated at other temperature ranges. At  $220^\circ\text{C}$ , molten nylon 6 underwent crystallization by using the un-molten nylon 6 crystals as nucleation center. Crystallization at higher temperature produced nylon 6 with the thicker crystalline lamella. The above results were helpful for rational design of the thermal treatment procedure so that nylon 6 with different crystalline features could be obtained.

## ACKNOWLEDGMENTS

This work was supported by the National Natural Science Foundation of China (NSFC51373003, NSFC50403026, NSFC20671007), National Research Center of the Polish Ministry of Science and Higher Education (Grant No. N N204 354840) and the financial support from Henan Province (2011B150015, 134300510054, 201310).

## REFERENCES

1. Gargalaka, J., Jr.; Couto, R. A. A.; Constantino, V. R. L.; Toma, H. E.; Araki, K. *J. Appl. Polym. Sci.* **2012**, *125*, 3239.
2. Wan, T.; Du, T.; Wang, B.; Zeng, W.; Clifford, M. *Polym. Compos.* **2012**, *33*, 2271.
3. Xia, G.; He, L.; Zhao, Q.; Chen, W.; Song, R.; Ma, Z. *Colloid Polym. Sci.* **2012**, *290*, 1943.
4. Liu, S.; Zhang, C.; Liu, Y.; Zhao, Y.; Xu, Y.; Ozaki, Y.; Wu, J. *J. Mol. Struct.* **2012**, *1021*, 63.
5. Kawabata, J.; Matsuba, G.; Nishida, K.; Inoue, R.; Kanaya, T. *J. Appl. Polym. Sci.* **2011**, *122*, 1913.
6. Cheng, S. Z. D.; Janimak, J. J.; Zhang, A.; Hsieh, E. T. *Polymer* **1991**, *32*, 648.
7. Mudra, I.; Balázs, G. *J. Therm. Anal. Calorim.* **1998**, *52*, 355.
8. Tol, R. T.; Mathot, V. B. F.; Groeninckx, G. *Polymer* **2005**, *46*, 383.
9. Tol, R. T.; Mathot, V. B. F.; Groeninckx, G. *Polymer* **2005**, *46*, 369.
10. Zhang, F.; Wang, B.; Man, R.; Peng, Z. *Polym. Eng. Sci.* **2014**, *54*, 2610.
11. Rafique, F. Z.; Vasanthan, N. *J. Phys. Chem. B* **2014**, *118*, 9486.
12. Chen, Y.; Zou, H.; Liang, M. *J. Polym. Res.* **2014**, *21*, 417.
13. Mileva, D.; Monami, A.; Cavallo, D.; Alfonso, G. C.; Portale, G.; Androsch, R. *Macromol. Mater. Eng.* **2013**, *298*, 938.
14. Liu, S.; Zhang, C.; Proniewicz, E.; Proniewicz, L. M.; Kim, Y.; Liu, J.; Zhao, Y.; Xu, Y.; Wu, J. *Spectrochim. Acta Part A* **2013**, *115*, 783.
15. Rwei, S.-P.; Tseng, Y.-C.; Chiu, K.-C.; Chang, S.-M.; Chen, Y.-M. *Thermochim. Acta* **2013**, *555*, 37.
16. Hemlata, S.; Maiti, N. *J. Polym. Res.* **2012**, *19*, 9926.
17. Cho, A.-R.; Shin, D. M.; Jung, H. W.; Hyun, J. C.; Lee, J. S.; Cho, D.; Joo, Y. L. *J. Appl. Polym. Sci.* **2011**, *120*, 752.
18. Guo, T.; Ding, X.; Han, H.; Zhang, L.; Zhang, Y.; Zhou, K. *J. Polym. Res.* **2012**, *19*, 9813.
19. Zhang, C.; Liu, Y.; Liu, S.; Li, H.; Huang, K.; Pan, Q.; Hua, X.; Hao, C.; Ma, Q.; Lv, C.; Li, W.; Yang, Z.; Zhao, Y.; Wang, D.; Lai, G.; Jiang, J.; Xu, Y.; Wu, J. *Sci. China Ser. B* **2009**, *52*, 1835.
20. Li, H.; Wu, Y.; Sato, H.; Kong, L.; Zhang, C.; Huang, K.; Tao, D.; Chen, J.; Liu, X.; Zhao, Y.; Xu, Y.; Wu, J.; Ozaki, Y. *Macromolecules* **2009**, *42*, 1175.
21. Pei, A. H.; Liu, A. D.; Xie, T. X.; Yang, G. S. *Macromolecules* **2006**, *39*, 7801.
22. Wunderlich, B. *Macromolecular Physics*, Ed.; Academic Press: New York, **1976**; Vol. 2, Crystal Nucleation, Growth, Annealing.
23. Zheng, T.; Zhou, Q.; Li, Q.; Li, H.; Zhang, L.; Hu, Y. *RSC Adv.* **2015**, *5*, 9328.
24. Cavallo, D.; Gardella, L.; Portale, G.; Mueller, A. J.; Alfonso, G. C. *Polymer* **2014**, *55*, 137.
25. Sun, X.; Shen, G.; Shen, H.; Xie, B.; Yang, W.; Yang, M. *J. Macromol. Sci. B* **2013**, *52*, 1372.
26. Joiode, A. S.; Hawkins, K.; Tonelli, A. E. *Macromol. Mater. Eng.* **2013**, *298*, 1190.
27. Chang, H.; Zhang, Y.; Ren, S.; Dang, X.; Zhang, L.; Li, H.; Hu, Y. *Polym. Chem.* **2012**, *3*, 2909.
28. Balzano, L.; Rastogi, S.; Peters, G. *Macromolecules* **2011**, *44*, 2926.
29. Pan, P.; Zhao, L.; Zhu, B.; He, Y.; Inoue, Y. *J. Appl. Polym. Sci.* **2010**, *117*, 3013.
30. Fillon, B.; Wittmann, J. C.; Lotz, B.; Thierry, A. *J. Polym. Sci. Polym. Phys.* **1993**, *31*, 1383.
31. Fillon, B.; Lotz, B.; Thierry, A.; Wittmann, J. C. *J. Polym. Sci. Polym. Phys.* **1993**, *31*, 1395.
32. Fillon, B.; Thierry, A.; Wittmann, J. C.; Lotz, B. *J. Polym. Sci. Polym. Phys.* **1993**, *31*, 1407.
33. Vanden Poel, G.; Mathot, V. B. F. *Thermochim. Acta* **2007**, *461*, 107.
34. Wunderlich, B. In *Thermal Analysis of Polymeric Materials*, Springer: Berlin Heidelberg, **2005**; 591.
35. Holmes, D. R.; Bunn, C. W.; Smith, D. J. *J. Polym. Sci.* **1955**, *17*, 159.
36. Arimoto, H.; Ishibashi, M.; Hirai, M.; Chatani, Y. *J. Polym. Sci., Part A* **1965**, *3*, 317.
37. Penel, L.; Depecker, C.; Séguéla, R.; Lefebvre, J. -M. *J. Polym. Sci. Polym. Phys.* **2001**, *39*, 484.
38. Lorenzo, A. T.; Arnal, M. L.; Muller, A. J.; de Fierro, A. B.; Abetz, V. *Macromol. Chem. Phys.* **2006**, *207*, 39.